Broadband Conductor Backed-CPW to Substrate Integrated Slab Waveguide Transition for Ku-Band

Anil Kumar Nayak
Dept. of Electrical and Computer Engg.
University of Alberta, Alberta, Canada
IIT Roorkee, Roorkee, India
aknayak@ualberta.ca

Igor M Filanosky
Dept. of Electrical and Computer Engg.
University of Alberta
Alberta, Canada
ifilanov@ualberta.ca

Kambiz Moez
Dept. of Electrical and Computer Engg.
University of Alberta
Alberta, Canada
kambiz@ualberta.ca

Amalendu Patnaik
Dept. of Electronics and Communication Engg.
IIT Roorkee
Roorkee, India
amalendu.patnaik@ece.iitr.ac.in

2022 IEEE Radio and Wireless Symposium (RWS) | 978-1-6654-3462-1/22/$31.00 ©2022 IEEE | DOI: 10.1109/RWS53089.2022.9719913

***Abstract*—The paper considers the transition from conductor backed coplanar waveguide (CB-CPW) to substrate integrated slab waveguide (SISW). The SISW concept is described, it improves the single-mode impedance bandwidth, reduces insertion loss, and the overall loss of the transition. Design example is presented for 12-18 GHz frequency range. The parameters of the transition laboratory prototype are measured to validate the claims.**

***Index Terms*—Broadband, CPW, Ku-band, substrate integrated slab waveguide.**

I. Introduction

Microwave circuits, using passive and active components, are widely used in various communication devices. The components such as transmission lines (TLs) antennas, filters, amplifiers, and transitions require compact size, low loss, high power handling, and low leakage loss. Conventional rectangular waveguide (CRW) as shown in Fig. 1(a), is preferred due to its high power handling capability [1], [2]. The CRW, however, is heavy, expensive, and requires transition for its operation. To address these issues, planar microstrip technology was introduced [3]. The microstrip components have such advantages as compactness, low-profile, light weight, and inexpensive fabrication. Yet, in the millimeter-wave (mm-wave) frequency range, the planar microstrip device has significant losses, more radiation leakage, undesired coupling between adjacent elements, and limited power handling capability. To resolve these issues, a new concept of substrate integrated waveguide (SIW) was introduced in 1998 [4]. This concept was implemented on planar technology in 2001 [5]. The RF components designed using SIW approach are more compact and lighter than the CRW ones [6]. In the mm-wave and THz frequency range, the SIW is also more advantageous than the planar microstrip because of its low loss, high-quality factor, wider bandwidth, and low interference [7].

To increase the impedance bandwidth and power handling capability, a new concept, the slab waveguide (SWG) was

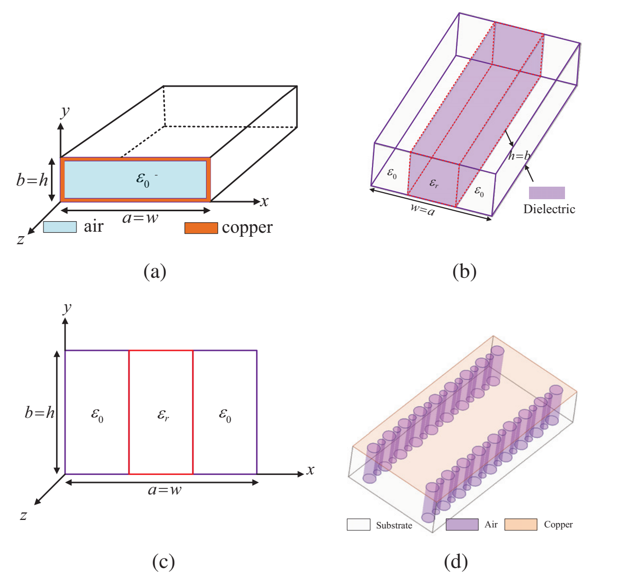

Fig. 1. Different types of guided structure, (a) Rectangular waveguide, (b) Dielectric waveguide (DWG), (c) Cross-section of DWG and (d) The DWG using air vias.

introduced in 1958 [8], as shown in Fig. 1(b) and (c). The operating principle of the SWG is the same as that of a dielectric waveguide (DWG) reported in [10], but it uses the air vias shown in Fig. 1 (d). The combination of the SIW and the air perforated DWG is known as substrate integrated slab waveguide (SISW). It uses metal vias as external wall and air vias to separate central part of the dielectric. The main objectives of SISW introduced in 2003 [9] and 2005 [10] were additional benefits such as easy fabrication, compactness, using substrate integrated transmission lines (TLs), and enhanced impedance bandwidth. The SISW propagates TE_{m0}-mode waves only. In [11], the SISW has provided approximately the doubled bandwidth compared to the metallic waveguide.

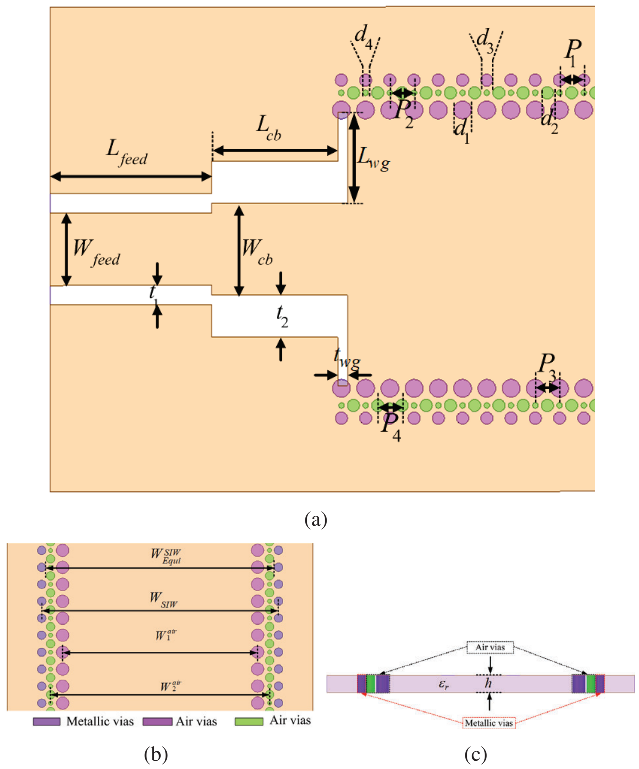

Fig. 2. The proposed transition: (a) top view, (b) the SISW part dimensions, (c) cross-section of SISW part.

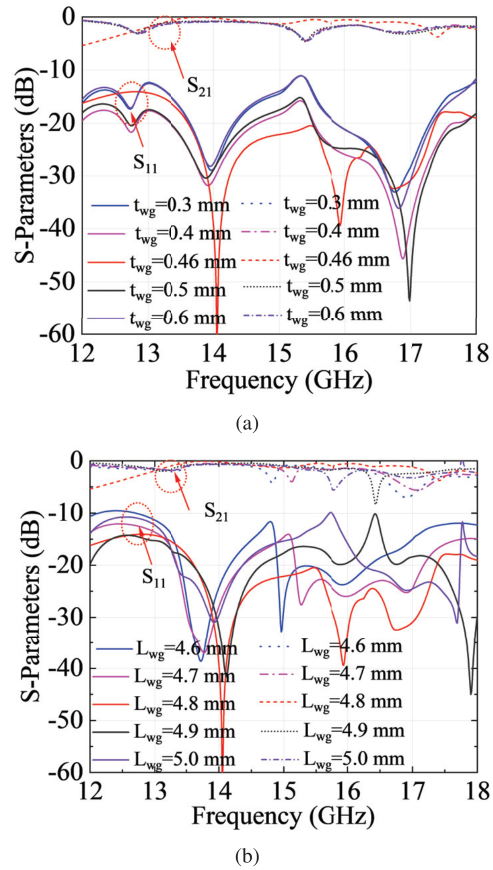

Fig. 3. Effect of t_{wg} (a) and L_{wg} (b) on S-parameters.

Recently, some applications using SISW concept, like filter [12], antenna [13], and transition [14] have been reported.

The principal objective of this work is to improve the single mode bandwidth from CB-CPW to SISW transition characteristics for the Ku-band application. At first, the structure was designed to use SIW at the Ku-band frequency range. After that, two air perforated rows of vias are implemented at two sides of the transition, which are parallel to each other. These rows of air filled vias reduced the dielectric density outside the central dielectric part of the structure. As a result, quasi TE_{10}-mode is practically unaffected since the electric field propagates in the middle part of SIW. Consequently, the transition also propagates the dominant mode (TE_{10}). The design is fabricated and tested in the laboratory. The simulated and measured results are in a good agreement.

II. Conductor Backed-CPW-to-SISW Transition

The design and working principle of the transition structure are explained better with two steps: (A) structure, and (B) working principle as follows.

A. Transition Structure

Fig. 2 shows the top, central part, and cross-sectional view of the proposed transition. The transition dimensions are $d_3 = 0.75$, $P_3 = 1.5$, $d_1 = 1.1$, $P_1 = 1.5$, $d_4 = 0.3375$, $P_4 = 1.5$, $d_2 = 0.75$, $P_2 = 1.5$, $L_{feed} = 4.5$, $W_{feed} = 10$ $t = 1.2$, $L_{cb} = 7.8$, $W_{cb} = 5.7$, $t_2 = 2.6$, $W_1^{air} = 15.225$, $W_2^{air} = 17.35$; unit: millimeters. Initially, the design was constructed using the SIW concept. Then, at each side, two additional air via rows were placed inside the metallic rows of vias, parallel to each other. This created SISW, and this design enhanced the single mode-impedance bandwidth (SM-IBW). The structure was implemented with the Rogers RO4232 material ($\varepsilon_r = 3.2$, $tan\delta = 0.0018$, and $h = 1.524$ mm) available in the laboratory. The main SISW dimensions, namely, the cut-off frequency f_c, the vias diameter d_3, and the pitch P_1, are found from the equations frequently used [5], [6], [15], [16] in SIW design as follows:

$$f_c = \frac{c}{2W^{SIW}_{Equi}\sqrt{\varepsilon_r}}; \lambda_g = \frac{\lambda_0}{\sqrt{\varepsilon_e}}; d_3 \leq \frac{\lambda_g}{5}; P_1 \leq 2d_3 \quad (1)$$

$$W^{Equi}_{SIW} = W_{SIW} - 1.08\frac{d_3^2}{P_1} + 0.1\frac{d_3^2}{W_{SIW}} \quad (2)$$

Here λ_g, is the guided wavelength at the center frequency, λ_0 is the wavelength in the free space or air, and ε_e is the effective relative dielectric constant of the substrate, c is the speed of light. The critical part of the transition design is the impedance matching between the feeding (Z_0) and the SISW (Z_L) parts. If (Z_L) is not equal to Z_0, the return loss will occur in the structure. To better match the feed and SISW parts, the middle section is added. The dimensions t_{wg} and L_{wg} (Fig. 2(a)) are playing a crucial role for the transition characteristics.

These dimensions were established by simulations, and the results are discussed in the next section. All simulations were carried out using electromagnetic software HFSS version 2020R2.

B. Working Principle

In the SISW structure (Fig. 2(a)), from each side, two rows of air vias are placed beside the row of metallic vias, and in parallel to the metallic row of vias. Due to presence of air vias, the effective relative dielectric constant is reduced in the structure. Even it affects only the side portion of the waveguide, the losses for dominant mode become smaller. The maximum electric field $\vec{E}$ can still be found at the middle of the transition (SISW part). Consequently, the rows of air vias allow to enhance the single-mode impedance bandwidth without affecting the TE_{10}-mode (dominant or fundamental mode). In this design, the desired cut off frequency f_c is taken at 9.65 GHz. The range of impedance bandwidth can be calculated as $1.25f_c$ to $1.9f_c$,, which is 12.06 to 18.33 GHz range.

To set the dimension of the length L_{wg} and the gap t_{wg}, the parametric analysis has been used. Fig. 3 (a) shows the results of parametric analysis when t_{wg} varies from 0.3 to 0.6 mm with a step of 0.1 mm. It can be noticed that S_{11} is slightly touching -10 dB line at t_{wg}=0.3 mm. When t_{wg} increases from 0.3 to 0.5 mm, the return loss (RL) goes above 15 dB, whereas the insertion loss (IL) is below 3 dB, and IL becomes more than 3 dB at 15.20 GHz with t_{wg} of 0.4 and 0.5 mm. When t_{wg} is set at 0.46 mm ($0.041\lambda_g$ at 15 GHz), RL is above 20 dB and IL is below 1.8 dB. These values were considered satisfactory, and t_{wg} =0.46 mm was chosen as the final dimension. The length L_{wg} was varied from 4.6 to 5.0 mm with a step of 0.1 mm. The simulation results are shown in Fig. 3 (b). The RL and IL are found the best in the simulation with the value of L_{wg} equal to 4.8 mm. Hence, L_{wg} is set at 4.8 mm ($0.42\lambda_g$ at 15 GHz). The electric field and the surface current distributions are calculated at 17.1 GHz. They are shown in Fig. 4(a) and (b), respectively.

III. Experimental Validation and Discussion

Fig. 5 shows the front and backside views of the fabricated prototype. Fig. 6(a) shows the S-parameters. The simulated

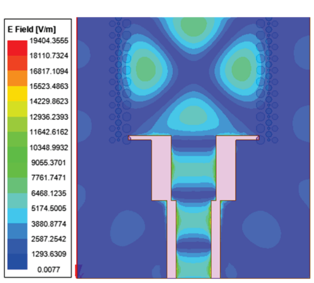

(a)

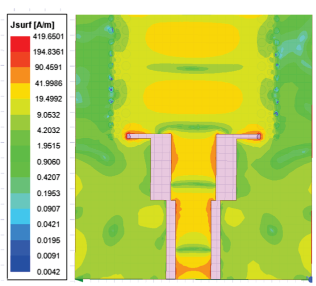

(b)

Fig. 4. The electric field (a) and the surface current (b) distributions at 17.1 GHz.

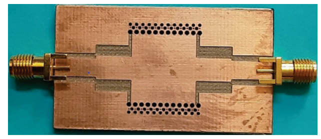

(a)

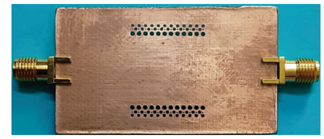

(b)

Fig. 5. PCB prototype of proposed transition: (a) front and (b) backside views.

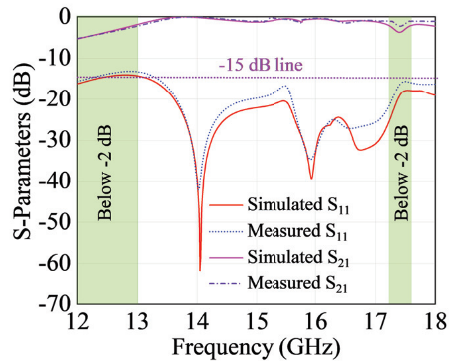

(a)

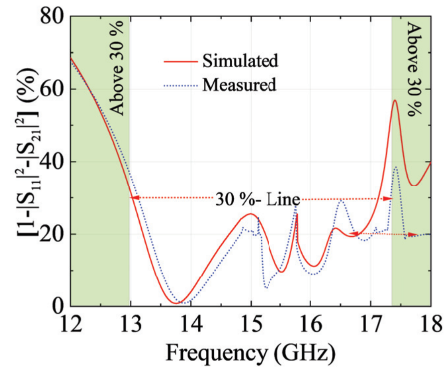

(b)

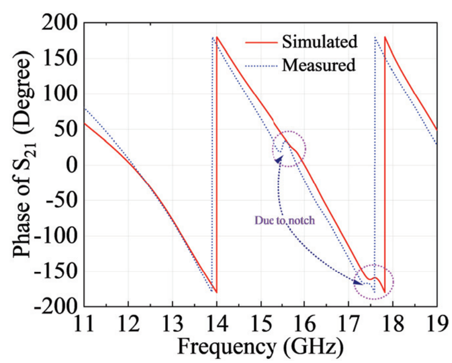

(c)

Fig. 6. Simulated and measured results: (a) $|S_{11}|$ and $|S_{21}|$ (b) total loss, and (c) phase of S_{21}.

and measured results of RL ($|S_{11}|$) are found above 15 dB. Similarly, the IL ($|S_{21}|$) is obtained below 1.8 dB except for two frequency ranges of 12-13 and 17.2-17.6 GHz. In these ranges, the IL is marked above 2 dB. To verify the overall losses ($1 - |S_{11}|^2 - |S_{21}|^2$) in these two frequency

TABLE I
COMPARISON OF COMPETITIVE BROADBAND TRANSITIONS TO SISW-SIW

Ref.	Frequency range	RL (dB)	IL (dB)	BW (GHz/%)
[17]	2.6-3.95	15	0.2	1.35/40.53
[18]	4-8	18.23	0.76	4/66.67
[19]	24.25-27.5	35	1.05	3.25/**NR**
This work	**12-18**	**15**	**1.8**	**6/40**

NR=Not reported

ranges, the simulated and measured results of overall losses have been plotted, as shown in Fig. 6(b). It can be observed from this plot, that the losses are below 30% in the whole band whereas in these two ranges (12-13 and 17.2-17.6 GHz) they are above 30%. The notches present in the experimental phase of S_{21} (Fig. 6 (c)) indicate on the power losses in the copper paste fillings of the vias. Yet, the measured results are in good agreement with the simulated ones.

Table I summarizes the performance of the proposed design, and gives comparison with the previously reported works. With the normal PCB process, it demonstrates that the proposed design functions at 12-18 GHz frequency range and has the benefits of easy fabrication, large BW (both GHz/%), and acceptable IL.

IV. Conclusion

In this paper, a broadband transition from CB-CPW to SISW is presented. To validate the design, the transition has been fabricated and measured at the Ku-band frequency range. The transition is suitable for different microwave applications.

V. Acknowledgment

We would like to acknowledge Science and Engineering Research Board, Govt. of India, for providing the financial support to carry out this research under the Overseas Visiting Doctoral Fellowship Award No. SB/S9/Z-16/2016-V (2019-20). We also thank Mr. S. Gaur and Mr. Kamveer for their assistance in the fabrication and measurements carried out in this work.

References

[1] D. M. Pozar, *Microwave Engineering, 3rd ed*. New York: Wiley, 2005.
[2] A. Weisshaar, M. Mongiardo, and V. Tripathi, “Cad-oriented equivalent circuit modeling of step discontinuities in rectangular waveguides,” *IEEE Microwave and Guided Wave Letters*, vol. 6, no. 4, pp. 171–173, 1996.
[3] R. Sorrentino, “Planar circuits, waveguide models, and segmentation method,” *IEEE Transactions on Microwave Theory and Techniques*, vol. 33, no. 10, pp. 1057–1066, 1985.
[4] A. Tugulea and I. R. Ciric, “Two-dimensional equations for microwave planar circuits,” in *1998 Symposium on Antenna Technology and Applied Electromagnetics*, 1998, pp. 315–318.
[5] D. Deslandes and K. Wu, “Integrated microstrip and rectangular waveguide in planar form,” *IEEE Microwave and Wireless Components Letters*, vol. 11, no. 2, pp. 68–70, 2001.
[6] D. Deslandes, “Design equations for tapered microstrip-to-substrate integrated waveguide transitions,” in *2010 IEEE MTT-S International Microwave Symposium*, 2010, pp. 704–707.
[7] Z. Kordiboroujeni and J. Bornemann, “New wideband transition from microstrip line to substrate integrated waveguide,” *IEEE Transactions on Microwave Theory and Techniques*, vol. 62, no. 12, pp. 2983–2989, 2014.
[8] W. Ayres, P. Vartanian, and A. Helgesson, “Propagation in dielectric slab loaded rectangular waveguide,” *IRE Transactions on Microwave Theory and Techniques*, vol. 6, no. 2, pp. 215–222, 1958.
[9] D. Deslandes, M. Bozzi, P. Arcioni, and K. Wu, “Substrate integrated slab waveguide (sisw) for wideband microwave applications,” in *IEEE MTT-S International Microwave Symposium Digest, 2003*, vol. 2, 2003, pp. 1103–1106 vol.2.
[10] M. Bozzi, D. Deslandes, P. Arcioni, L. Perregrini, K. Wu, and G. Conciauro, “Efficient analysis and experimental verification of substrate-integrated slab waveguides for wideband microwave applications,” *International Journal of RF and Microwave Computer-Aided Engineering*, vol. 15, no. 3, pp. 296–306, 2005.
[11] E. Massoni, L. Silvestri, G. Alaimo, S. Marconi, M. Bozzi, L. Perregrini, and F. Auricchio, “3-d printed substrate integrated slab waveguide for single-mode bandwidth enhancement,” *IEEE Microwave and Wireless Components Letters*, vol. 27, no. 6, pp. 536–538, 2017.
[12] N.-H. Nguyen, A. Ghiotto, T.-P. Vuong, A. Vilcot, T. Martin, and K. Wu, “Dielectric slab air-filled substrate integrated waveguide (safsiw) bandpass filters,” *IEEE Microwave and Wireless Components Letters*, vol. 30, no. 4, pp. 363–366, 2020.
[13] Z. Qi, X. Li, J. Xiao, and H. Zhu, “Dielectric-slab-loaded hollow substrate-integrated waveguide h-plane horn antenna array at ka-band,” *IEEE Antennas and Wireless Propagation Letters*, vol. 18, no. 9, pp. 1751–1755, 2019.
[14] H. Peng, F. Zhao, Y. Liu, S. O. Tatu, and T. Yang, “Robust microstrip to empty substrate-integrated waveguide transition using tapered artificial dielectric slab matrix,” *IEEE Microwave and Wireless Components Letters*, vol. 30, no. 9, pp. 849–852, 2020.
[15] A. K. Nayak, R. Pachpole, and A. Patnaik, “Compact symmetric quarter mode substrate integrated waveguide (qmsiw) antenna,” in *2018 IEEE Indian Conference on Antennas and Propagation (InCAP)*, 2018, pp. 1–4.
[16] A. K. Nayak, V. S. Yadav, and A. Patnaik, “Design and testing of a broadband microstrip line-empty siw transition for 5g applications,” in *2021 XXXIVth General Assembly and Scientific Symposium of the International Union of Radio Science (URSI GASS)*, 2021, pp. 1–4.
[17] R.-Y. Fang, C.-F. Liu, and C.-L. Wang, “Compact and broadband cb-cpw-to-siw transition using stepped-impedance resonator with 90 degree-bent slot,” *IEEE Transactions on Components, Packaging and Manufacturing Technology*, vol. 3, no. 2, pp. 247–252, 2013.
[18] A. Kumar Nayak and A. Patnaik, “Design and testing of a broadband microstrip-siw transition,” in *2020 IEEE Microwave Theory and Techniques in Wireless Communications (MTTW)*, vol. 1, 2020, pp. 91–95.
[19] A. G. Garca, Y. Campos-Roca, R. G. Alcal, and J. Rubio, “Multistep transitions from microstrip and gcpw lines to siw in 5g 26 ghz band,” *IEEE Access*, vol. 9, pp. 68 778–68 787, 2021.